Petroleum Science 20 (2023) 3184–3193

Contents lists available at ScienceDirect

Petroleum Science

journal homepage: www.keaipublishing.com/en/journals/petroleum-science

Original Paper

Numerical study of inhibition mechanism of high-pressure hydrogen leakage self-ignition with the addition of ammonia

Lin Teng [a, b], Xi-Gui Li [a], Zhi-Wei Shan [a], Wei-Dong Li [a, b], Xin Huang [a, *], Peng-Bo Yin [a], Yong-Zhen Liu [d], Jiang Bian [c], Yu Luo [a, b], Li-Long Jiang [a, b, **]

[a] National Engineering Research Center of Chemical Fertilizer Catalyst (NERC-CFC), College of Chemical Engineering, Fuzhou University, Fuzhou, 350000, Fujian, China
[b] Qingyuan Innovation Laboratory (QYIL, Fujian Innovation Laboratory of Chemical Engineering), Quanzhou, 362000, Fujian, China
[c] College of Pipeline and Civil Engineering, China University of Petroleum (East China), Qingdao, 266580, Shandong, China
[d] State Key Laboratory of Automobile Safety and Energy, School of Vehicle and Mobility, Tsinghua University, Beijing, 100084, China

ARTICLE INFO

Article history:
Received 22 November 2022
Received in revised form
24 March 2023
Accepted 26 March 2023
Available online 30 March 2023

Edited by Jia-Jia Fei

Keywords:
Ammonia-hydrogen energy
Self-ignition
Shock waves
Diffusion ignition
Computational fluid dynamics

ABSTRACT

Hydrogen and ammonia have attracted increasing attention as carbon-free fuels. Ammonia is considered to be an effective energy storage and hydrogen storage medium. However, a small amount of unremoved NH_3 is still present in the product during the decomposition of ammonia to produce hydrogen. Therefore, it is very essential to investigate the self-ignition of hydrogen-ammonia mixtures in order to accommodate the various scenarios of hydrogen energy applications. In this paper, the effect of NH_3 addition on the self-ignition of high-pressure hydrogen release is numerically investigated. The RNG k-ε turbulence model, EDC combustion model, and 213-step detailed NH_3/H_2 combustion mechanism are used. CHEMKIN-Pro programs for zero-dimensional homogeneous and constant volume adiabatic reactor models are used for sensitivity analysis and ignition delay time of the chemical reaction mechanism. The results showed that the minimum burst pressure required for self-ignition increased significantly after the addition of ammonia. The maximum temperature and shock wave intensity inside the tube decreases with increasing ammonia concentration. The ignition delay time and H, HO_2, and OH radicals reduce with increasing ammonia concentration. H and HO_2 radicals are suggested as indicators for tracking the second and third flame branches, respectively.

1. Introduction

Hydrogen has been considered as the most future energy due to its clean, environmental protection, low carbon, and other advantages (Gielen et al., 2019; Zhu et al., 2022a). At present, high-pressure storage by gaseous hydrogen is the most widespread method for hydrogen storage with relatively simple and inexpensive technology (Usman, 2022). However, high-pressure tanks may cause uncontrolled hydrogen release due to tank bursts, punctures, tank overheating, etc. (Rudy et al., 2017). High-pressure hydrogen leakage into the air without clearly identifiable ignition sources may cause self-ignition, which will further lead to jet fires, explosions, etc. (Zhang et al., 2020).

In recent years, some scholars had proposed five hypothetical inferences for the mechanism of hydrogen self-ignition (Astbury and Hawksworth, 2007): (1) Reverse Joule-Thomson effect, (2) Hot surface ignition, (3) Sudden adiabatic compression, (4) Electrostatic ignition, and (5) Diffusion ignition. Of these mechanisms, diffusion ignition is widely accepted and researched by current researchers.

Recently, many scholars have investigated the numerous factors causing hydrogen self-ignition based on the diffusion ignition mechanism. The study found that hydrogen self-ignition was influenced by the boundary layer (Asahara et al., 2014; Xu et al., 2020), the diameter of the tube and its length (Duan et al., 2018; Jin et al., 2021; Kitabayashi et al., 2013), the release pressure (Asahara et al., 2022; Duan et al., 2019), the tube cross-section (Asahara et al., 2023; Li et al., 2019), the tube with different inlet

* Corresponding author.
** Corresponding author. National Engineering Research Center of Chemical Fertilizer Catalyst (NERC-CFC), College of Chemical Engineering, Fuzhou University, Fuzhou, China.
E-mail addresses: huangxin@fzu.edu.cn (X. Huang), jll@fzu.edu.cn (L.-L. Jiang).

https://doi.org/10.1016/j.petsci.2023.03.025

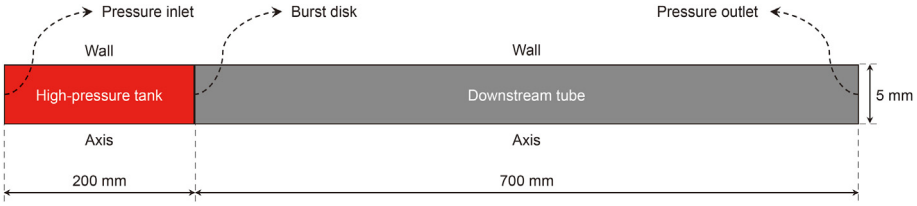

Fig. 1. Geometric model of the experimental setup.

Table 1
Boundary conditions.

Parameters	Boundary condition
Inlet	Pressure-inlet boundary
Outlet	Pressure-outlet boundary
Inlet species	Pure hydrogen
Burst disk	Interior, open instantaneously
Tank and tube top wall	No slip wall, adiabatic boundary
Tank and tube lower wall	Axis
Temperature, K	300

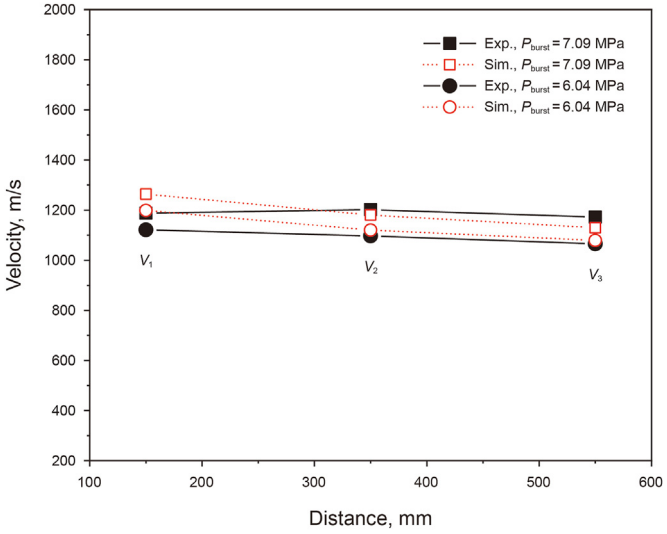

Fig. 2. Comparison of experiment and simulation.

shapes (Zhang et al., 2022), the diaphragm process (Asahara et al., 2021; Gong et al., 2019a; Kaneko and Ishii, 2016), the geometries of the downstream tube (Gong et al., 2016; Jin et al., 2022; Li et al., 2021b; Pan et al., 2020; Wang et al., 2020a, 2020b; Xu and Wen, 2014), and the obstacles inside the pipeline (Li et al., 2021a, 2022; Morii et al., 2015), etc. To further reveal the pattern of self-ignition occurrence and flame propagation when hydrogen was suddenly released into the downstream pipeline. Kim et al. (2013) completely documented the formation of self-ignition flame in the rectangular transparent tube and discovered that self-ignition occurs first in the boundary layer, and then the flame propagates along the boundary layer toward the front and tail of the mixing zone.

The above-mentioned study investigated the self-ignition of pure hydrogen. However, the future scenarios of hydrogen energy applications are becoming more and more diverse. Therefore, some scholars have investigated the influence of adding other gases on hydrogen self-ignition. For instance, several scholars have experimentally investigated the effects of adding methane (CH_4) (Rudy et al., 2014; Zeng et al., 2020a, 2020b), carbon dioxide (CO_2) (Gong et al., 2019b), nitrogen (N_2) (Rudy et al., 2017; Zeng et al., 2022a), and carbon monoxide (CO) (Zeng et al., 2022b) on the high-pressure hydrogen self-ignition. They discovered that the self-ignition of high-pressure hydrogen was effectively suppressed by the addition of CH_4, CO_2, N_2, and CO. To further reveal the micro-kinetic properties of the effect of gas addition on hydrogen self-ignition. Zhong and Gou. (2021) revealed the diffusion ignition of a pressurized H_2/CH_4 jet produced by the accidental release through numerical simulation methods. Although several scholars have investigated the effect of adding inert (N_2, CO_2, CO) or combustible (CH_4) gases on hydrogen self-ignition, there is still a serious lack of studies on the effect of other combustible gases on the self-ignition of hydrogen. In particular, there are few reports in the field of numerical simulation. At present, H_2 and NH_3 have attracted increasing attention as carbon-free fuels (Sun et al., 2022). In the ammonia-hydrogen energy roadmap for carbon neutrality, hydrogen was produced by the decomposition of ammonia, and a small amount of unremoved NH_3 was still present in the product stream (Jiang and Fu, 2021). However, there is a lack of analytical studies on the influence of NH_3 addition on hydrogen self-ignition. Therefore, it is essential to study the effect of adding NH_3 on high-pressure hydrogen self-ignition.

Some researchers took the OH mole fraction >0.001 as the criterion for the occurrence of high-pressure hydrogen self-ignition (Bragin et al., 2013; Bragin and Molkov, 2011; Gong et al., 2020). In addition, OH radicals were used to identify the flame front. However, the indicator for tracking the flame front may change

Table 2
Major parameters in numerical simulations.

Name	Parameters
Domain	2D-axis
Solver	Double-precision, pressure-based, transient
Mixture gas	Ideal gas
Thermal conductivity, viscosity, and density	Ideal-gas-mixing-law
Turbulent model	RNG k-ε model
Combustion model	Species transport with finite-rate model and EDC combustion model
Chemical reaction kinetic mechanism	213-step NH_3/H_2 reaction mechanism
Discretization scheme	Pressure–velocity coupling, PISO algorithm, the second-order upwind scheme
Time step, s	10^{-9}
Ignition delay time, normalized sensitivity	Constant volume zero-dimensional homogeneous adiabatic reactor

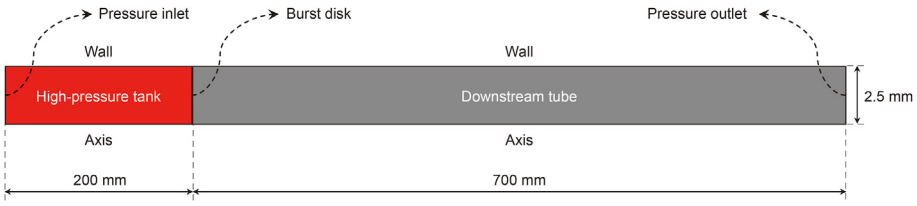

Fig. 3. Physical model.

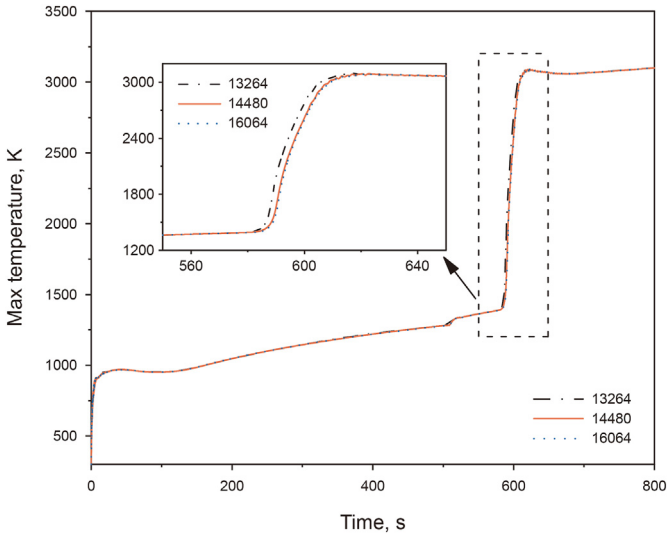

Fig. 4. Grid-independence analysis.

when other gases were added. For instance, Zhu et al. (2022b) compared the evolution of the OH radical, H radical, HO_2 radical, and heat release rates (HRR), noting that the H radical had a good trend of change with HRR and recommended the H radical as an indicator to indicate the flame front. In addition, Zhong and Gou. (2021) also considered the OH and HO_2 radicals as good indicators for tracking the branching flame of hydrogen self-ignition. The results show that at low mixture fractions, OH radicals indicate a diffusion flame, and at high mixture fractions, HO radicals indicate a partially premixed flame. In summary, the indicators capturing the branch flame of hydrogen self-ignition may change after the addition of ammonia to hydrogen.

To further reveal the influence of ammonia addition on hydrogen self-ignition. In this work, a two-dimensional axisymmetric model was developed based on the computational fluid dynamics (CFD) approach. The RNG k-ε turbulence model, the Eddy Dissipation Concept (EDC) model, and the 213-step detailed combustion reaction kinetic mechanism are used. The influence of ammonia addition on hydrogen self-ignition and shock wave propagation is numerically investigated. In addition, species tracking the flame front are discussed. As well, a sensitivity analysis of the chemical reaction mechanism is performed.

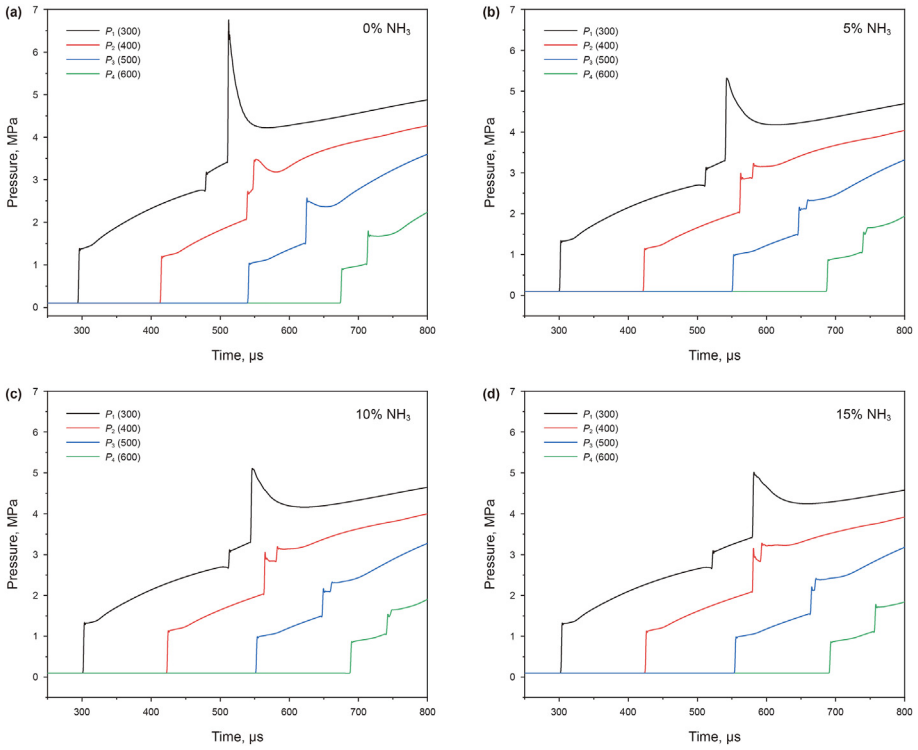

Fig. 5. The pressure curves for different concentrations of NH_3 addition inside the tubes.

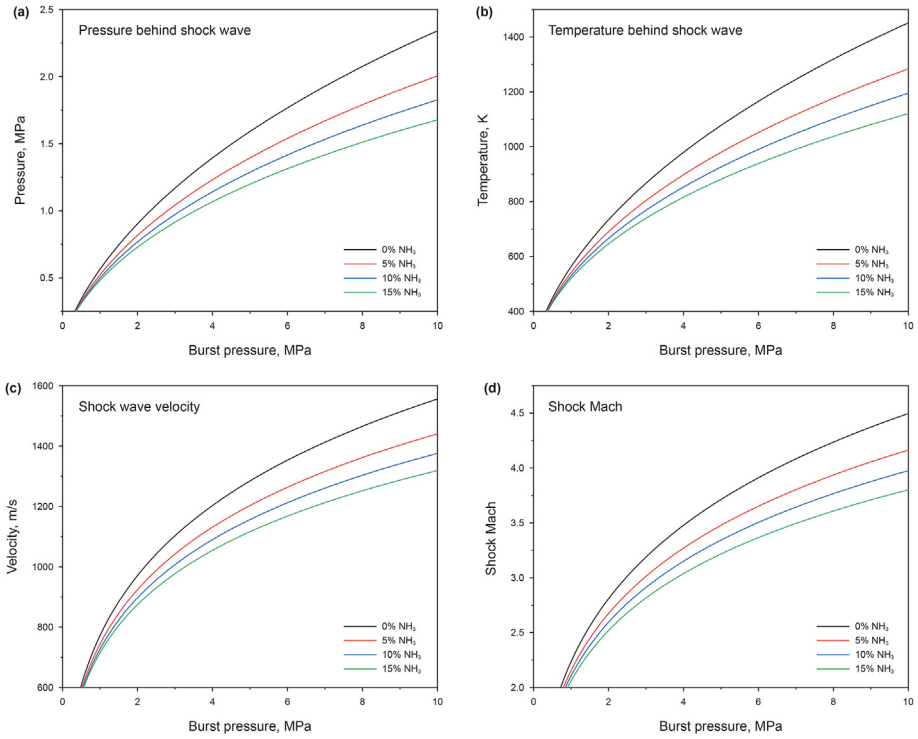

Fig. 6. Theoretical pressure, temperature, and shock Mach behind the shock wave and shock wave velocity.

2. Numerical methods

2.1. Numerical schemes

At present, there are no experimental and simulation studies on the influence of ammonia addition on hydrogen self-ignition. Therefore, the high-pressure hydrogen self-ignition experiment by Xu et al. (2020) was chosen to validate the model. Since phenomena such as hydrogen self-ignition and shock wave propagation occur only in the downstream tube, the high-pressure tank in the simulation was simplified as in Xu et al. (2020). The computational domain was shown in Fig. 1. After the grid-independent simulation, a grid with 27075 cells was used in the subsequent calculation. The boundary conditions used in the simulations were summarized in Table 1.

In this work, Fluent 18.0 was used as the calculation tool and the finite volume method was employed to solve the 2D-axis Unsteady Reynolds Averaged Navier-Stokes (URANS) equations for a compressible Newtonian fluid. The 213-step detailed chemical reaction kinetic mechanism (Otomo et al., 2018) was chosen to simulate the chemical reaction of NH_3/H_2 in air and handle

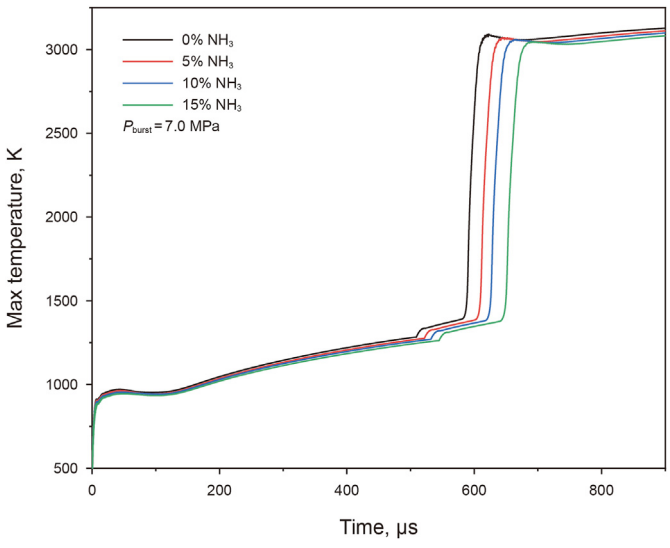

Fig. 7. Variation of the maximum temperature inside the tube with different ammonia concentration additions.

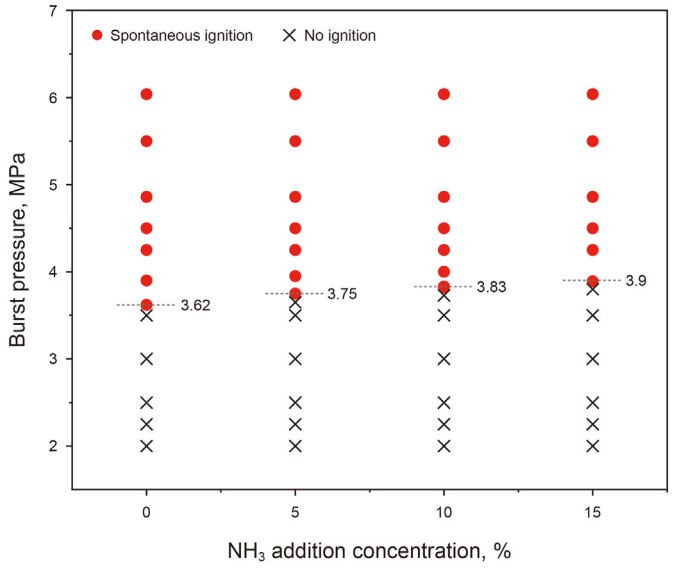

Fig. 8. Burst pressure for self-ignition to occur at different NH_3 concentration additions.

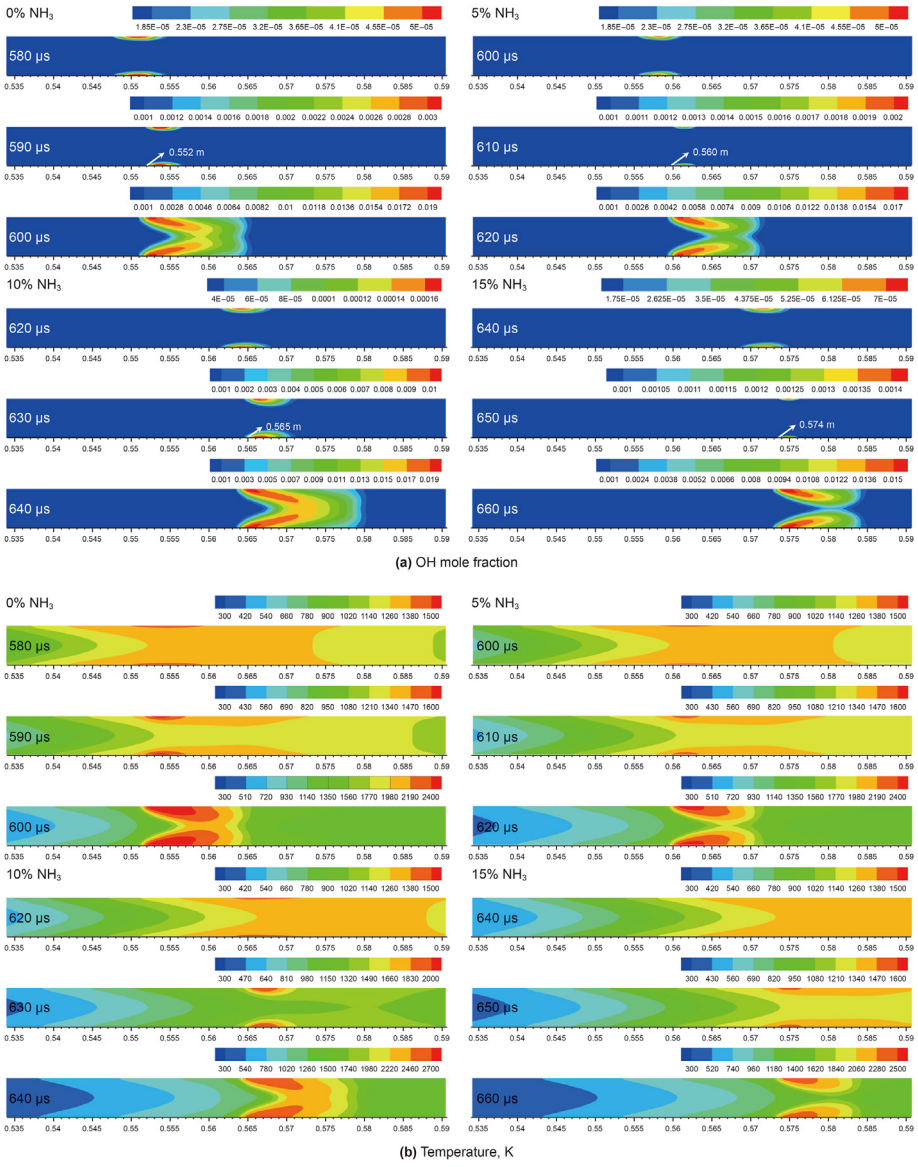

Fig. 9. The contour of OH mole fraction and temperature during self-ignition with different NH_3 concentration additions (P_{burst}: 7.0 MPa; Units: meter).

turbulence-chemistry interactions. Moreover, this mechanism contains a detailed H_2/O_2 chemical reaction mechanism. The species transport with the finite-rate model (Fluent, 2011) and EDC combustion model (Magnussen, 1981) were employed to handle the combustion reactions whereas the RNG k-ε model (Yakhot and Orszag, 1986) was employed to simulate both high and low Reynolds number turbulence. For details see our previous paper (Li et al., 2022). To further explain the 213-step NH_3/H_2 chemical reaction kinetic mechanism, numerical simulations were carried out using the CHEMKIN-Pro program (Kee et al., 1996). A zero-dimensional (0-D) adiabatic reactor model with a constant volume was used. The numerical simulation details were summarized in Table 2.

2.2. Model validation

Fig. 2 shows the comparison between the numerical simulation results and the experimental data. The results show that the simulation results were in good agreement with the experimental data. In this work, hydrogen was considered the ideal gas, and the burst disk was considered to rupture instantaneously. Therefore, the V_1 of the numerical simulation was always greater than the V_1 of the experimental results in the initial stage of the high-pressure hydrogen leakage, regardless of the burst pressure. When the burst pressure was relatively low (P_{burst} = 6.04 MPa), the shock wave intensity weakened and the shock wave velocity decreased accordingly due to the dissipation and attenuation of the shock wave (Xu et al., 2020). Therefore, the shock wave velocity was gradually reduced for both the numerical simulation and the experimental process. However, the numerically simulated shock wave velocity reduction trend was much faster. This was due to the superposition of compressional waves generated during the multi-stage rupture of the experimental burst disk which makes the shock wave velocity decrease slowly.

When the burst pressure was high (P_{burst} = 7.09 MPa), the compressional waves produced by the burst disk's multi-stage rupture process would have a significant superimposed effect and increase the propagation velocity of the shock waves (Asahara et al., 2021; Gong et al., 2019a; Kaneko and Ishii, 2016). Therefore, at

P_{burst} = 7.09 MPa, the experimental V_2 was larger than the numerical simulation V_2. After the rupture, the shock wave decays steadily, and the shock wave velocity gradually decreases. As a result, during the experiment, the shock wave's propagation velocity first rises and then gradually falls. However, in the numerical simulation, the velocity of the shock wave was always decreasing gradually. In conclusion, V_3 of the numerical simulation was smaller than V_3 of the experiment. In summary, there was a small discrepancy between the simulation results and the experimental results. In addition, the maximum average relative error between the numerical simulation results and the experimental data was 3.93%. Therefore, the CFD model used in this paper was correctly validated.

2.3. Model description

Researchers at the Warsaw University of Technology indicated that the self-ignition of high-pressure hydrogen was related to the length of the tube, but not to the diameter of the tube (Rudy et al., 2014, 2017). Therefore, the effect of diameter on hydrogen self-ignition was neglected in this work, and the self-ignition of high-pressure hydrogen in a 700 mm long tube with a diameter of 5 mm was investigated. The above-mentioned validated CFD model was used for simulations to study the effect of ammonia addition (0, 5, 10, and 15%) on the self-ignition of high-pressure hydrogen leakage. Fig. 3 shows the schematic diagram of the physical model. To ensure grid-independent simulations, a grid-independent analysis was performed by using several grid counts. It was found that the simulation results for the maximum temperature evolution (P_{burst} = 7.0 MPa) changed very little when the number of grids was increased from 14480 to 16064, as shown in Fig. 4. Thus, the total number of grids eventually used was 14480.

3. Result and discussion

3.1. Effects of ammonia concentration on shock wave inside the tube

Fig. 5 shows the pressure curves at different locations in the tube for various ammonia concentration additions (The distances of P_1, P_2, P_3, and P_4 from the burst disk are 300 mm, 400 mm, 500 mm, and 600 mm, respectively). The four cases have the same burst pressures of 8.50 MPa but have different NH_3 additions of 0%, 5%, 10%, and 15%. From Fig. 5, a sudden increase in pressure is successively detected by the four pressure monitoring points at the tube wall. It suggests that after the burst disk opens, a leading shock wave is produced and propagates along the downstream tube. Moreover, from Fig. 5(a)–(d), it is observed that the pressure in the tube gradually reduces with the increase of NH_3 concentration, which will inhibit the occurrence of self-ignition.

According to the usual one-dimension (1-D) shock tube theory (Gaydon and Hurle, 1963), the theoretical Mach number (M), pressure behind the shock wave (P_2), the temperature behind the shock wave (T_2), and shock wave velocity can be obtained in Eqs. (1)–(4):

$$\frac{P_4}{P_1}=\frac{2\gamma_1 M^2-(\gamma_1-1)}{\gamma_1+1}\left[1-\frac{\gamma_4-1}{\gamma_1+1}\frac{a_1}{a_4}\left(M-\frac{1}{M}\right)\right]^{-2\gamma_4/(\gamma_4-1)} \quad (1)$$

$$a_4=(\gamma_4 RT_4/M)^{1/2} \quad (2)$$

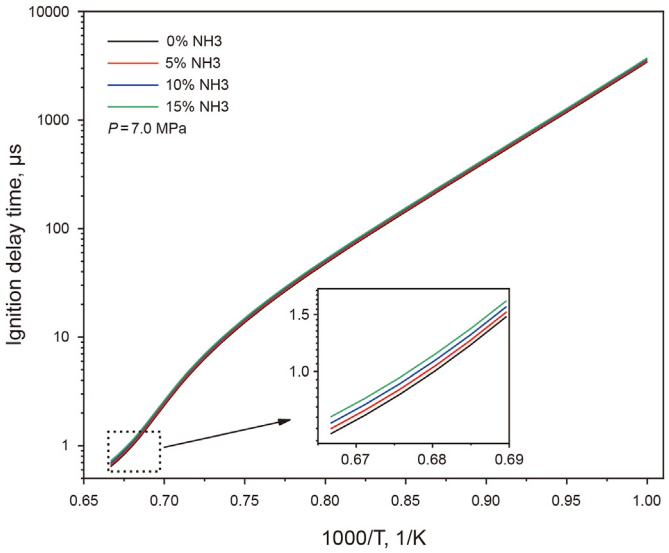

Fig. 10. Ignition delay times of H_2/NH_3/air with different ammonia concentration additions.

$$\frac{P_2}{P_1}=\frac{2\gamma_1 M^2-(\gamma_1-1)}{\gamma_1+1} \quad (3)$$

$$\frac{T_2}{T_1}=\frac{\left[2\gamma_1 M^2-(\gamma_1-1)\right]\left[(\gamma_1-1)M^2+2\right]}{(\gamma_1+1)^2 M^2} \quad (4)$$

where P_4 is the initial pressure in the high-pressure region, and P_1 is the initial pressure in the tube. T_1 and T_4 are the initial temperature in the tube and high-pressure region, respectively. r_1 and r_4 is the gas-specific heat ratio of air and ammonia/hydrogen mixture, respectively. a_1 and a_4 is the speed of sound in air and hydrogen/ammonia mixture, respectively. According to Eq. (1), the addition of NH_3 affects the values of a_4 and r_4 in the mixture. Since the heat capacity ratios of the three gases (air, hydrogen, ammonia) are similar, the change in the heat capacity ratio of the mixture at

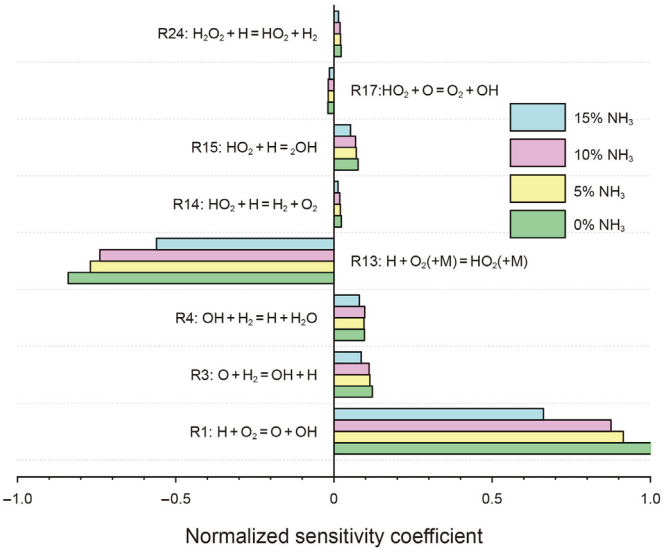

Fig. 11. Normalized sensitivity analysis of ignition delay time for various NH_3/H_2 mixtures at 1500 K and 7.0 MPa.

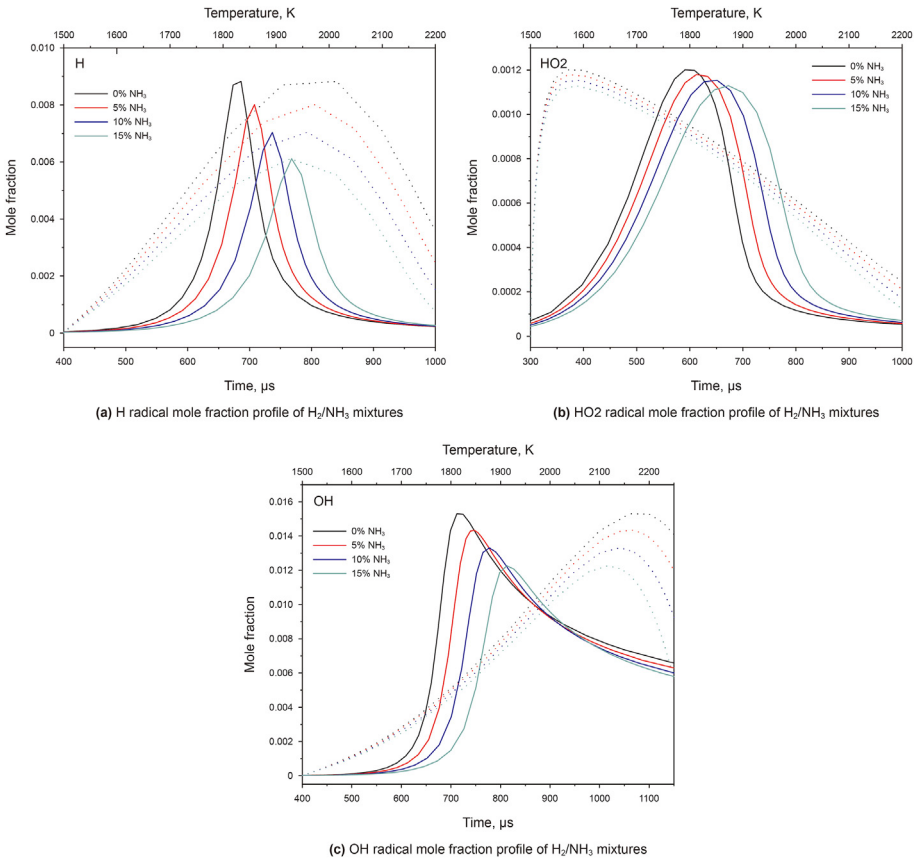

(a) H radical mole fraction profile of H_2/NH_3 mixtures

(b) HO2 radical mole fraction profile of H_2/NH_3 mixtures

(c) OH radical mole fraction profile of H_2/NH_3 mixtures

Fig. 12. H, OH, and HO_2 radical mole fraction profiles of hydrogen/ammonia mixture at 1600 K, 7.0 MPa, $Z_{mr} = 0.01$ (The solid line represents change with time; the dotted line represents change with temperature).

different ratios of hydrogen is negligible. However, the sonic speed in hydrogen/ammonia mixture with different NH_3 additions can be calculated as Eq. (2). In hydrogen/ammonia mixtures, increasing the concentration of ammonia will reduce the local sound speed. Fig. 6(a) shows the theoretical shock wave velocity for different concentrations of ammonia added to high-pressure hydrogen. Fig. 6(a), the shock wave velocity reduces as ammonia is added. Analogously, based on the 1-D shock tube theory, the pressure, temperature, and shock Mach behind the shock wave are displayed in Fig. 6(b), (c), and (d), respectively. The results show that the pressure, temperature, and shock Mach behind the shock wave reduce as more ammonia is added to the high-pressure hydrogen.

3.2. Effects of ammonia addition on self-ignition inside the tube

Fig. 7 shows the effect of different NH_3 concentration additions on the maximum temperature inside the tube. From Fig. 7, it can be found that the maximum temperature profiles for different NH_3 concentrations have a similar trend. The maximum temperature profile for 15% NH_3 concentration addition is used as an example. After the instantaneous rupture of the burst disk, the leading shock wave generated in the tube makes the first increase in the tube temperature within 0–38 μs. At 38–645 μs, the temperature inside the tube gradually increased with the propagation of the leading shock wave to the downstream tube. At 645–683 μs, when self-ignition takes place in the tube after the temperature jumps to about 3000 K in a very short period. At 683–725 μs, the temperature increases slightly and then decreases slightly. After that, the temperature will gradually increase with time, which indicates the formation of a stable hydrogen flame in the tube. Moreover, as the NH_3 concentration increase, the maximum temperature inside the tube gradually decreased, and the occurrence time of self-ignition is gradually delayed.

Fig. 8 shows the minimum burst pressure for self-ignition to occur at different NH_3 concentration additions. In this work, the OH mole fraction >0.001 is considered a criterion for the occurrence of self-ignition (Bragin et al., 2013; Bragin and Molkov, 2011; Gong et al., 2020; Jin et al., 2021; Zhang et al., 2020). From Fig. 8, the minimum burst pressure of self-ignition to occur for 0% NH_3 is 3.62 MPa. However, for 5%, 10%, and 15% NH_3 addition, the values increase to 3.75, 3.83, and 3.90 MPa, respectively, which are 1.036, 1.058, and 1.077 times higher than in the case of 0%. The results show that the addition of ammonia will significantly improve the critical burst pressure for high-pressure hydrogen self-ignition to occur.

Fig. 9 shows the contour of OH mole fraction and temperature during self-ignition with different NH_3 concentration additions. As shown in Fig. 9, the initial self-ignition happens in the boundary layer at different NH_3 concentration additions. Then, the flame propagates around the boundary layer and reaches the front and tail of the mixing zone. Finally, a complete flame is formed around the mixing zone and moves downstream with the shock wave. However, when NH_3 concentration is added at 0%, 5%, 10%, and 15%, the distances between the burst disk and the location of self-ignition occurrence are about 0.552, 0.560, 0.565, and 0.574 m, respectively. Moreover, the self-ignition onset times were 590, 610, 630, and 650 μs, respectively. Therefore, as the NH_3 concentration increases, the possibility of self-ignition occurs gradually decreases.

3.3. Effect of NH_3 addition on the chemical kinetic mechanism

The initial mass ratio of fuel versus air in the H_2/NH_3/air mixture is programmed to be higher than the most reactive mixture fraction ($Z_{mr} = 0.01$) (Zhong and Gou, 2021). Fig. 10 shows the ignition delay time (IDT) versus the initial temperature for H_2/NH_3/air mixtures added with different ammonia concentrations. The initial pressure and initial temperature of the reactor are 7.0 MPa and 1000–1600 K, respectively. The results show that the ignition delay time of the H_2/NH_3 binary fuel decreases exponentially as the initial temperature increases. Moreover, the ignition delay time gradually increases with the NH_3 concentration increases, but the increase is not significant. This interesting phenomenon is similar to the influence of CH_4 adding on the self-ignition of pressurized hydrogen studied by Zhong and Gou (2021). Therefore, the results show that the addition of NH_3 has not caused significant changes in the high-pressure hydrogen ignition mechanism.

Fig. 11 shows the normalized sensitivity coefficient of the stoichiometric H_2/NH_3 mixture to the ignition delay time. A positive coefficient indicates that the response has a positive effect on the ignition delay time and vice versa. The initial temperature is 1500 K, the constant pressure is 7.0 MPa, and the mixing levels are 0, 0.05, 0.1, and 0.15. As shown in Fig. 11, the ignition delay time is strongly influenced by the chain-branching reactions $H+O_2 = O+OH$ (R1) and $H+O_2 (+M) = HO_2 (+M)$ (R13). Moreover, under current conditions, the chain-branching reaction R1 is always the most significant chain-branching reaction producing many reactive radicals (O and OH), and also the most significant chain-branching reaction promoting the combustion of all hydrogen/ammonia mixtures. In contrast, the chain-branching reaction R13 has an obvious negative effect on the ignition delay time. This is because the chain-branching reaction R13 consumes the H radical and produces the stable intermediate radical HO_2. In addition, the sensitivity coefficients of all chain-branching reactions decrease with increasing the proportion of ammonia. Thus, the sensitivity of ignition delay time decreases gradually with increasing ammonia concentration.

3.4. Evolution of OH, HO_2, H, and HRR

As discussed in the sensitivity analysis above, the H, HO_2, and OH radicals have a significant effect on the chain-branching reaction during hydrogen ignition; therefore, it is necessary to investigate the effect of ammonia addition on the mole fractions of H, HO_2, and OH radicals. Meanwhile, the H, OH, and HO_2 radicals are strongly associated with hydrogen ignition. Fig. 12 shows the mole fraction profiles of H, HO_2, and OH radicals for different stoichiometric H_2/NH_3 mixtures. The initial temperature is 1500 K, the initial pressure is 7.0 MPa, and $Z_{mr} = 0.01$. From Fig. 12, the peak of H, HO_2, and OH radicals decreased with increasing the proportion of ammonia. In addition, the H and HO_2 radicals decreased more significantly compared to the HO_2 radicals. In conclusion, the addition of ammonia decreases the accumulation of OH, HO_2, and H radicals.

In addition, studies by several scholars have shown that OH, HO_2, and H radicals could all capture the ignition kernel (Zhong and Gou, 2021; Zhu et al., 2022b). Therefore, in this section, indicators that can be used to track the flame branches of hydrogen self-ignition are investigated. Fig. 13 shows the variation of HRR, OH radicals, HO_2 radicals, and H radicals on the central axis of the tubes for different NH_3 concentrations. As shown in Fig. 13, compared to OH radical, the trends of H and HO_2 radicals mole fractions are more similar to the trends of HRR. It is found that the H and HO_2 radicals show three peak concentration accumulations inside the tube, which indicates that three separate flames are produced.

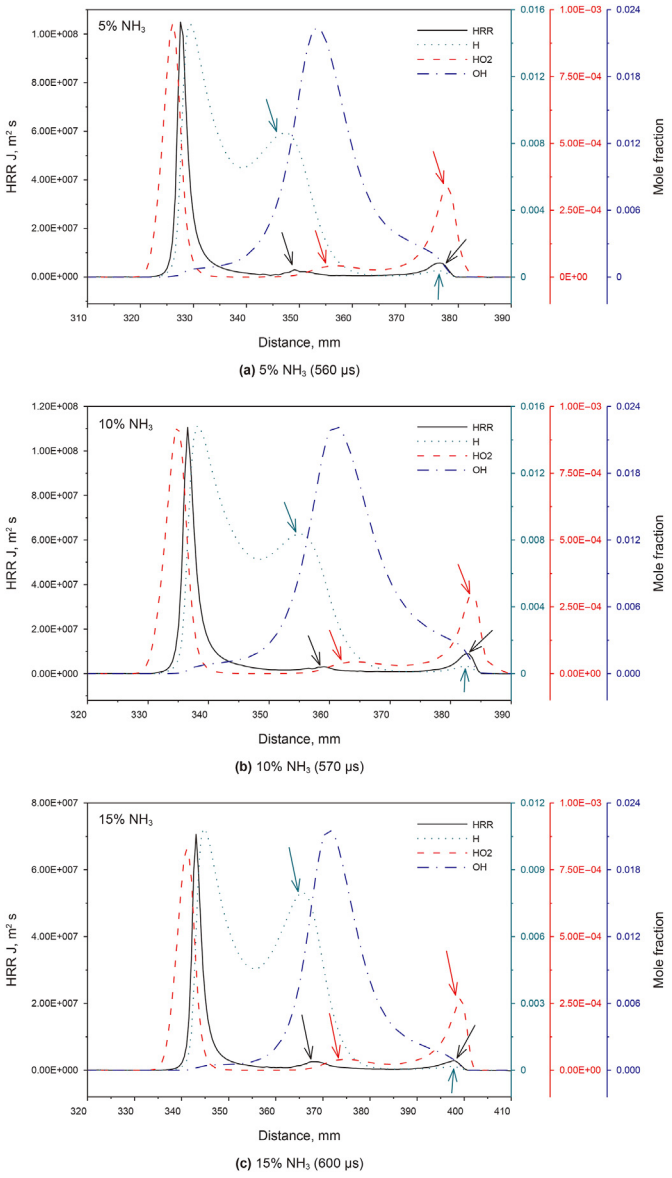

Fig. 13. HRR and mole fraction of H, HO_2, and OH radicals on the central axis in tubes of different NH_3 concentrations additions ($P_{burst} = 8.5$ MPa).

However, the OH radical showed only one peak concentration accumulation in the tube and could not show three separate flames. As shown in Fig. 13(a)–(c), it is found that the second peak concentration accumulations of H radicals are more obvious than the H and HO_2 radicals. Yet, the third peak concentration accumulations of the HO_2 radical are more obvious than the OH and H radicals. Therefore, the flame branches cannot be captured by only one of the OH, H, or HO_2 radicals. The results show that H and HO_2 radicals are good indicators for tracking the second and third flame branches, respectively, compared to OH radicals. At the same time, it can be observed that the peak of OH is in front of the peak of HRR. This is because in a shock tube-like channel where the air is in the low-pressure side and the fuel mixture will break the diaphragm, OH radicals will be formed in the front (heated gases are in the front when shock wave passed through), and because the fuel is behind the shock front, the flame will propagate against the propagation direction of the fuel gas mixture. Therefore, OH peaks in front of the HRR.

4. Conclusions

In this paper, the effect of NH_3 concentration additions (0%, 5%, 10%, and 15%) on the self-ignition of high-pressure hydrogen accidently released into the tube is numerically investigated. The species transport with finite-rate model and EDC combustion model is employed to study the combustion reactions whereas the RNG k-ε model is used for the turbulence model, and the 213-step detailed hydrogen/ammonia chemical reaction kinetic mechanism is used. The mechanism of the effect of ammonia addition on the shock wave propagation, self-ignition occurrence, and combustion characteristics during the hydrogen self-ignition is elucidated. Moreover, the CHEMKIN-Pro program with the 0-D homogeneous and constant volume adiabatic reactor model performs a sensitivity analysis of the ignition delay time of the combustion reaction mechanism. The following conclusions are drawn.

(1) The intensity and propagation velocity of the shock wave in the tube reduced with the increase of NH_3 concentration. Based on the 1-D shock theory, the shock wave intensity decreases and the temperature of the shock wave heating decreases accordingly, which is detrimental to the occurrence of self-ignition. The value of the critical burst pressure required for self-ignition to occur increases with the addition of NH_3 concentration. In addition, the possibility of self-ignition decreased with increasing NH_3 concentration when the burst pressure is higher than the critical minimum burst pressure required for self-ignition to occur. Compared to the case of pure hydrogen, the critical burst pressure required for self-ignition may be increased by a factor of 1.036, 1.058, and 1.077 times for 5%, 10%, and 15% ammonia additions, respectively. As the concentration of NH_3 increases, the maximum temperature inside the tube gradually decreases and the onset of self-ignition is gradually delayed. With the increase of NH_3 concentration, the distance between the position where self-ignition occurs inside the tube and the burst disk gradually increases. However, regardless of the amount of ammonia added, the self-ignition inside the tube occurred at the tube wall.

(2) Further explanation of the effect of NH_3 addition on the combustion kinetic mechanism of the H_2/NH_3 chemical reaction is provided. The ignition delay time gradually increases with increasing NH_3 concentration. The ignition delay time is most affected by the chain-branching reaction $H+O_2 = O+OH$ (R1), which promoted the combustion of the hydrogen/ammonia mixture. The chain-branching reaction $H+O_2 (+M) = HO_2 (+M)$ (R13) has a significant negative effect on the ignition delay time, and the R13 plays a role in inhibiting self-ignition. The sensitivity coefficients for all chain-branching reactions decreased with increasing the proportion of NH_3. Therefore, the sensitivity of ignition delay time gradually reduces with the increase of NH_3 concentration.

(3) The effect of ammonia addition on the flame propagation characteristics is investigated. The accumulation of OH radicals, H radicals, and HO_2 radicals decreases with increasing the proportion of NH_3. Three peak concentration accumulations are observed for the mole fraction profiles of H and HO_2 radicals, which indicated the generation of three separate flames. The mole fraction trends of HO_2 and H radicals are more similar to those of HRR than those of OH radicals. Therefore, H and HO_2 radicals are suggested as good indicators for tracking the flame branches of hydrogen self-ignition compared to OH radicals. Moreover, based on the observed distinctness of the flame branches, H and HO_2 radicals are suggested as better indicators for tracking the second and third flame branches, respectively.

Declaration of competing interest

The authors declare that they have no known competing financial interests or personal relationships that could have appeared to influence the work reported in this paper.

Acknowledgments

The present work is supported by the National Key R&D Program of China for Renewable Energy and Hydrogen Technology (Grant No. 2021YFB4000403), the National Natural Science Foundation of China (Grant No. 52204072), the National Natural Science Foundation of China (Grant No. 22038002), the Science Fund for Creative Research Groups of the National Natural Science Foundation of China (Grant No. 22221005), the Fujian Science and Technology Major Project (Grant No. 2020HZ07009), and the Natural Science Foundation of Fujian Province (Grant No. 2020J05098).

References

Asahara, M., Saburi, T., Ando, T., Muto, T., Takahashi, Y., Miyasaka, T., 2022. Jet flame sustenance via spontaneous release of high-pressure hydrogen through a seamless tube: relationship between burst pressure and tube length. Fuel 315, 123228. https://doi.org/10.1016/j.fuel.2022.123228.

Asahara, M., Saburi, T., Ando, T., Takahashi, Y., Miyasaka, T., Kubota, S., 2021. Self-ignited flame behavior of high-pressure hydrogen release by rupture disk through a long tube. Int. J. Hydrogen Energy 46 (24), 13484–13500. https://doi.org/10.1016/j.ijhydene.2021.01.097.

Asahara, M., Yokoyama, A., Hayashi, A.K., Yamada, E., Tsuboi, N., 2014. Numerical simulation of auto-ignition induced by high-pressure hydrogen release with detailed reaction model: fluid dynamic effect by diaphragm shape and boundary layer. Int. J. Hydrogen Energy 39 (35), 20378–20387. https://doi.org/10.1016/j.ijhydene.2014.05.136.

Asahara, M., Yokoyama, A., Tsuboi, N., Hayashi, A.K., 2023. Influence of tube cross-section geometry on high-pressure hydrogen-flow-induced self-ignition. Int. J. Hydrogen Energy 48 (21), 7909–7926. https://doi.org/10.1016/j.ijhydene.2022.08.210.

Astbury, G., Hawksworth, S.J., 2007. Spontaneous ignition of hydrogen leaks: a review of postulated mechanisms. Int. J. Hydrogen Energy 32 (13), 2178–2185. https://doi.org/10.1016/j.ijhydene.2007.04.005.

Bragin, M.V., Makarov, D.V., Molkov, V.V., 2013. Pressure limit of hydrogen spontaneous ignition in a T-shaped channel. Int. J. Hydrogen Energy 38 (19), 8039–8052. https://doi.org/10.1016/j.ijhydene.2013.03.030.

Bragin, M.V., Molkov, V.V., 2011. Physics of spontaneous ignition of high-pressure hydrogen release and transition to jet fire. Int. J. Hydrogen Energy 36 (3), 2589–2596. https://doi.org/10.1016/j.ijhydene.2010.04.128.

Duan, Q., Xiao, H., Gong, L., Jin, K., Gao, W., Chai, H., Sun, J., 2018. Experimental study on spontaneous ignition and subsequent flame development caused by high-pressure hydrogen release: coupled effects of tube dimensions and burst pressure. Fire Saf. J. 97, 44–53. https://doi.org/10.1016/j.firesaf.2018.03.001.

Duan, Q., Xiao, H., Gong, L., Li, P., Zeng, Q., Gao, W., Sun, J., 2019. Experimental study of shock wave propagation and its influence on the spontaneous ignition during high-pressure hydrogen release through a tube. Int. J. Hydrogen Energy 44 (40), 22598–22607. https://doi.org/10.1016/j.ijhydene.2019.06.166.

Fluent, A., 2011. Ansys Fluent Theory Guide. ANSYS Inc., USA.

Gaydon, A.G., Hurle, I.R., 1963. The Shock Tube in High-Temperature Chemical Physics. Chapman and Hall, London.

Gielen, D., Boshell, F., Saygin, D., Bazilian, M.D., Wagner, N., Gorini, R., 2019. The role of renewable energy in the global energy transformation. Energy Strategy Rev. 24, 38–50. https://doi.org/10.1016/j.esr.2019.01.006.

Gong, L., Duan, Q., Jiang, L., Jin, K., Sun, J., 2016. Experimental study on flow characteristics and spontaneous ignition produced by pressurized hydrogen release through an Omega-shaped tube into atmosphere. Fuel 184, 770–779. https://doi.org/10.1016/j.fuel.2016.07.078.

Gong, L., Duan, Q., Liu, J., Li, M., Jin, K., Sun, J., 2019a. Effect of burst disk parameters on the release of high-pressure hydrogen. Fuel 235, 485–494. https://doi.org/10.1016/j.fuel.2018.08.044.

Gong, L., Duan, Q., Liu, J., Li, M., Jin, K., Sun, J., 2019b. Experimental investigation on effects of CO2 additions on spontaneous ignition of high-pressure hydrogen during its sudden release into a tube. Int. J. Hydrogen Energy 44 (13), 7041–7048. https://doi.org/10.1016/j.ijhydene.2019.01.197.

Gong, L., Jin, K., Yang, S., Yang, Z., Li, Z., Gao, Y., Zhang, Y., 2020. Numerical study on the mechanism of spontaneous ignition of high-pressure hydrogen in the L-shaped tube. Int. J. Hydrogen Energy 45 (56), 32730–32742. https://doi.org/10.1016/j.ijhydene.2020.08.267.

Jiang, L., Fu, X., 2021. An ammonia–hydrogen energy roadmap for carbon neutrality: opportunity and challenges in China. Engineering 7 (12), 1688–1691. https://doi.org/10.1016/j.eng.2021.11.004.

Jin, K., Yang, S., Gong, L., Han, Y., Yang, X., Gao, Y., Zhang, Y., 2021. Numerical study on the spontaneous ignition of pressurized hydrogen during its sudden release into the tube with varying lengths and diameters. J. Loss Prev. Process. Ind. 72, 104592. https://doi.org/10.1016/j.jlp.2021.104592.

Jin, K., Yang, S., Gong, L., Mo, T., Gao, Y., Zhang, Y., 2022. Mechanism of spontaneous ignition of high-pressure hydrogen during its release through a tube with local contraction: a numerical study. Int. J. Hydrogen Energy 47 (9), 6421–6436. https://doi.org/10.1016/j.ijhydene.2021.11.223.

Kaneko, W., Ishii, K., 2016. Effects of diaphragm rupturing conditions on self-ignition of high-pressure hydrogen. Int. J. Hydrogen Energy 41 (25), 10969–10975. https://doi.org/10.1016/j.ijhydene.2016.04.211.

Kee, R.J., Rupley, F.M., Meeks, E., Miller, J.A., 1996. CHEMKIN-III: A FORTRAN Chemical Kinetics Package for the Analysis of Gas-phase Chemical and Plasma Kinetics. Sandia National Lab.(SNL-CA), Livermore, CA (United States). https://doi.org/10.2172/481621.

Kim, Y.R., Lee, H.J., Kim, S., Jeung, I.-S., 2013. A flow visualization study on self-ignition of high pressure hydrogen gas released into a tube. Proc. Combust. Inst. 34 (2), 2057–2064. https://doi.org/10.1016/j.proci.2012.07.020.

Kitabayashi, N., Wada, Y., Mogi, T., Saburi, T., Hayashi, A.K., 2013. Experimental study on high pressure hydrogen jets coming out of tubes of 0.1–4.2 m in length. Int. J. Hydrogen Energy 38 (19), 8100–8107. https://doi.org/10.1016/j.ijhydene.2012.10.040.

Li, P., Duan, Q., Zeng, Q., Jin, K., Chen, J., Sun, J., 2019. Experimental study of spontaneous ignition induced by sudden hydrogen release through tubes with different shaped cross-sections. Int. J. Hydrogen Energy 44 (42), 23821–23831. https://doi.org/10.1016/j.ijhydene.2019.07.083.

Li, P., Zeng, Q., Duan, Q., Sun, J., 2021a. Visualization of spontaneous ignition and flame behavior in tubes with and without obstacles during the high-pressure hydrogen release. Process Saf. Environ. Protect. 153, 354–362. https://doi.org/10.1016/j.psep.2021.07.036.

Li, X., Teng, L., Li, W., Huang, X., Li, J., Luo, Y., Jiang, L., 2022. Numerical simulation of the effect of multiple obstacles inside the tube on the spontaneous ignition of high-pressure hydrogen release. Int. J. Hydrogen Energy 47 (77), 33135–33152. https://doi.org/10.1016/j.ijhydene.2022.07.202.

Li, Y., Jiang, Y., Pan, X., Wang, Z., Hua, M., Wang, Q., Ta, L., Jiang, J., 2021b. Effects of the arc-shaped corner on the shock wave and self-ignition induced by sudden release of pressurized hydrogen. Fuel 303, 121294. https://doi.org/10.1016/j.fuel.2021.121294.

Magnussen, B., 1981. On the Structure of Turbulence and a Generalized Eddy Dissipation Concept for Chemical Reaction in Turbulent Flow, 19th Aerospace Sciences Meeting, p. 42. https://doi.org/10.2514/6.1981-42.

Morii, Y., Terashima, H., Koshi, M., Shimizu, T., 2015. Numerical study of the effect of obstacles on the spontaneous ignition of high-pressure hydrogen. J. Loss Prev. Process. Ind. 34, 92–99. https://doi.org/10.1016/j.jlp.2015.01.020.

Otomo, J., Koshi, M., Mitsumori, T., Iwasaki, H., Yamada, K., 2018. Chemical kinetic modeling of ammonia oxidation with improved reaction mechanism for ammonia/air and ammonia/hydrogen/air combustion. Int. J. Hydrogen Energy 43 (5), 3004–3014. https://doi.org/10.1016/j.ijhydene.2017.12.066.

Pan, X., Wang, Q., Yan, W., Jiang, Y., Wang, Z., Xu, X., Hua, M., Jiang, J., 2020. Experimental study on pressure dynamics and self-ignition of pressurized hydrogen flowing into the L-shaped tubes. Int. J. Hydrogen Energy 45 (7), 5028–5038. https://doi.org/10.1016/j.ijhydene.2019.11.161.

Rudy, W., Dabkowski, A., Teodorczyk, A., 2014. Experimental and numerical study on spontaneous ignition of hydrogen and hydrogen-methane jets in air. Int. J. Hydrogen Energy 39 (35), 20388–20395. https://doi.org/10.1016/j.ijhydene.2014.05.077.

Rudy, W., Teodorczyk, A., Wen, J., 2017. Self-ignition of hydrogen–nitrogen mixtures during high-pressure release into air. Int. J. Hydrogen Energy 42 (11), 7340–7352. https://doi.org/10.1016/j.ijhydene.2016.06.051.

Sun, C., Fan, X., Li, Y., Han, H., Zhu, J., Liu, L., Geng, X., 2022. Research on the offshore adaptability of new offshore ammonia-hydrogen coupling storage and transportation technology. Renew. Energy 201, 700–711. https://doi.org/10.1016/j.renene.2022.11.017.

Usman, M.R., 2022. Hydrogen storage methods: review and current status. Renew. Sustain. Energy Rev. 167, 112743. https://doi.org/10.1016/j.rser.2022.112743.

Wang, Q., Pan, X., Jiang, Y., Wang, Z., Li, Y., Ta, L., Hua, M., Jiang, J., 2020a. Experimental investigation on spontaneous ignition caused by pressurized hydrogen suddenly release into an S-shaped tube. J. Loss Prev. Process. Ind. 68. https://doi.org/10.1016/j.jlp.2020.104313.

Wang, Z., Pan, X., Jiang, Y., Wang, Q., Li, Y., Xiao, J., Jordan, T., Jiang, J., 2020b. Experimental study on shock wave propagation and spontaneous ignition induced by high-pressure hydrogen suddenly released into T-shaped tubes. Saf. Sci. 127. https://doi.org/10.1016/j.ssci.2020.104694.

Xu, B.P., Wen, J.X., 2014. The effect of tube internal geometry on the propensity to spontaneous ignition in pressurized hydrogen release. Int. J. Hydrogen Energy 39 (35), 20503–20508. https://doi.org/10.1016/j.ijhydene.2014.04.141.

Xu, X., Jiang, J., Jiang, Y., Wang, Z., Wang, Q., Yan, W., Pan, X., 2020. Spontaneous ignition of high-pressure hydrogen and boundary layer characteristics in tubes. Int. J. Hydrogen Energy 45 (39), 20515–20524. https://doi.org/10.1016/j.ijhydene.2020.02.060.

Yakhot, V., Orszag, S.A., 1986. Renormalization group analysis of turbulence. I. Basic theory. J. Sci. Comput. 1 (1), 3–51. https://doi.org/10.1007/BF01061452.

Zeng, Q., Duan, Q., Jin, K., Zhu, M., Sun, J., 2022a. Effects of nitrogen addition on the shock-induced ignition of high-pressure hydrogen release through a rectangular tube of 400 mm in length. Fuel 308, 122016. https://doi.org/10.1016/j.fuel.2021.122016.

Zeng, Q., Duan, Q., Li, P., Zhu, H., Sun, D., Sun, J., 2020a. An experimental study of the effect of 2.5% methane addition on self-ignition and flame propagation during high-pressure hydrogen release through a tube. Int. J. Hydrogen Energy 45 (4), 3381–3390. https://doi.org/10.1016/j.ijhydene.2019.11.155.

Zeng, Q., Duan, Q., Sun, D., Li, P., Zhu, M., Wang, Q., Sun, J., 2020b. Experimental study of methane addition effect on shock wave propagation, self-ignition and flame development during high-pressure hydrogen sudden discharge from a tube. Fuel 277, 118217. https://doi.org/10.1016/j.fuel.2020.118217.

Zeng, Q., Jin, K., Duan, Q., Zhu, M., Gong, L., Wang, Q., Sun, J., 2022b. Effects of CO addition on shock wave propagation, self-ignition, and flame development of high-pressure hydrogen release into air. Int. J. Hydrogen Energy 47 (32), 14714–14724. https://doi.org/10.1016/j.ijhydene.2022.02.192.

Zhang, T., Jiang, Y., Pan, X., Wang, Z., Wang, Q., Li, Y., Ta, L., Hua, M., Jiang, J., 2022. Effects of tubes with different inlet shapes on the shock wave and self-ignition induced by accidental release of pressurized hydrogen. Fuel 317, 123554. https://doi.org/10.1016/j.fuel.2022.123554.

Zhang, Y., Chen, R., Zhao, M., Luo, J., Feng, W., Fan, W., Tan, Y., Cao, W., Shu, C., Yu, C., 2020. Hazard evaluation of explosion venting behaviours for premixed hydrogen-air fuels with different bursting pressures. Fuel 268, 117313. https://doi.org/10.1016/j.fuel.2020.117313.

Zhong, C., Gou, X., 2021. Inhibition mechanism of CH_4 addition on the pressurized hydrogen spontaneous ignition. Energy Fuel. 35 (2), 1715–1726. https://doi.org/10.1021/acs.energyfuels.0c03282.

Zhu, L., Li, Y., Liu, J., He, J., Wang, L., Lei, J., 2022a. Recent developments in high-performance Nafion membranes for hydrogen fuel cells applications. Petrol. Sci. 19 (3), 1371–1381. https://doi.org/10.1016/j.petsci.2021.11.004.

Zhu, M., Jin, K., Duan, Q., Zeng, Q., Sun, J., 2022b. Numerical simulation on the spontaneous ignition of high-pressure hydrogen release through a tube at different burst pressures. Int. J. Hydrogen Energy 47 (18), 10431–10440. https://doi.org/10.1016/j.ijhydene.2022.01.081.